

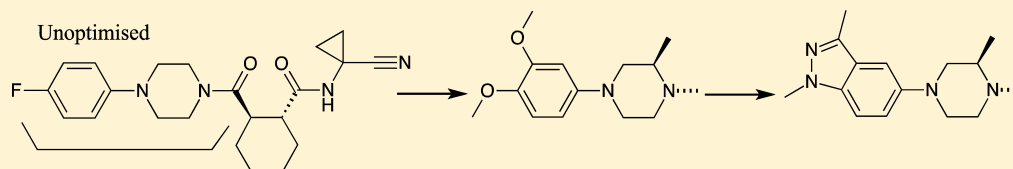
Pharmacokinetic Benefits of 3,4-Dimethoxy Substitution of a Phenyl Ring and Design of Isosteres Yielding Orally Available Cathepsin K Inhibitors

James J. Crawford,^{*,†,§,||} Peter W. Kenny,[†] Jonathan Bowyer,[†] Calum R. Cook,[†] Jonathan E. Finlayson,[†] Christine Heyes,[†] Adrian J. Highton,[†] Julian A. Hudson,[†] Anja Jestel,[‡] Stephan Krapp,[‡] Scott Martin,[†] Philip A. MacFaul,[†] Benjamin P. McDermott,[†] Thomas M. McGuire,[†] Andrew D. Morley,[†] Jeffrey J. Morris,[†] Ken M. Page,[†] Lyn Rosenbrier Ribeiro,[†] Helen Sawney,[†] Stefan Steinbacher,[‡] Caroline Smith,[†] and Alexander G. Dossetter^{*,†,||}

[†]AstraZeneca R&D, Mereside, Alderley Park, Macclesfield, Cheshire SK10 4TG, United Kingdom

[‡]Proteros Biostructures, Am Klopferspitz 19, D-82152 Martinsried, Germany

S Supporting Information



ABSTRACT: Rational structure-based design has yielded highly potent inhibitors of cathepsin K (Cat K) with excellent physical properties, selectivity profiles, and pharmacokinetics. Compounds with a 3,4-(CH₃O)₂Ph motif, such as **31**, were found to have excellent metabolic stability and absorption profiles. Through metabolite identification studies, a reactive metabolite risk was identified with this motif. Subsequent structure-based design of isosteres culminated in the discovery of an optimized and balanced inhibitor (indazole, **38**).

■ INTRODUCTION

The lysosomal cysteine protease cathepsin K (Cat K) is highly expressed in osteoclasts and plays a key role in bone resorption by the degradation of type I cartilage.¹ Cat K knockout mice exhibit osteopetrosis (abnormally dense bone) and abnormal joint morphology,² indicating the potential role of this enzyme in key bone pathologies such as osteoporosis (OP), osteoarthritis (OA), and metastatic bone disease (MBD).^{3–5} Osteoarthritis is a group of degenerative disorders, characterized by joint pain and loss of function in the absence of chronic autoimmune or autoinflammatory mechanisms.⁶ They have an increasing prevalence with age and are thus a growing socioeconomic burden.² Articular cartilage breakdown is a prominent feature of joint degeneration and, as a result, has received significant attention from the pharmaceutical industry. Several companies have trialed compounds in the OP and OA disease areas. Novartis has completed phase II studies in OP and OA with balicatib (**1**; Figure 1).⁷ The phase II OP trial reported positive outcomes on bone mineral density measures. Merck has completed a phase III trial in OP with odanacatib (**2**; Figure 1); the trial was stopped early as both safety and primary efficacy (reduced bone fracture risk) end points were reached.^{8–11} Both compounds are electrophilic nitrile-containing compounds that bind covalently and reversibly to the Cat K enzyme, preventing type I collagen degradation. We have previously described efforts that led to the identification of

AZD4996 (**3**), a potent and selective inhibitor of Cat K with good pharmacokinetic properties,¹² and the thiazolopiperazine **4** from the phenyl compound **5** (Figure 1), where increasing the margin to hERG inhibition was improved.¹³ Herein we describe the discovery of **5** and the development of the *N*-phenylpiperazinyl series of compounds.

Drug Hunting Approach. During our initial investigations, which led to the discovery of **3**, it was also found that *N*-phenylpiperazinyl-containing compounds were an attractive alternative series. While not as potent inhibitors as their carboline counterparts, the (4-fluorophenyl)piperazine compound **5**, also made in that first library, was only 20-fold less active.¹² The binding of **5** was confirmed by solving an X-ray structure complex (PDB 4DMX; Figure 2A). The nitrile bound covalently to Cys25 in the P1 region, part of the Cys–Asn–His triad, within the active site of the protein.¹⁴ The alkyl nitrile “warhead” of **1–5**, which forms this covalent bond,^{15,16} has the advantage of being less electrophilic than nitriles attached to heteroaromatic rings such as pyrimidine.^{17,18} The attached amide was well positioned for protein backbone donor–acceptor interactions,¹⁹ and the *trans*-cyclohexyldiamide scaffold was a good fit in the P2 pocket (Figure 2B).²⁰ The remaining amide portion (phenylpiperazinyl) of the molecule

Received: July 31, 2012

Published: September 17, 2012

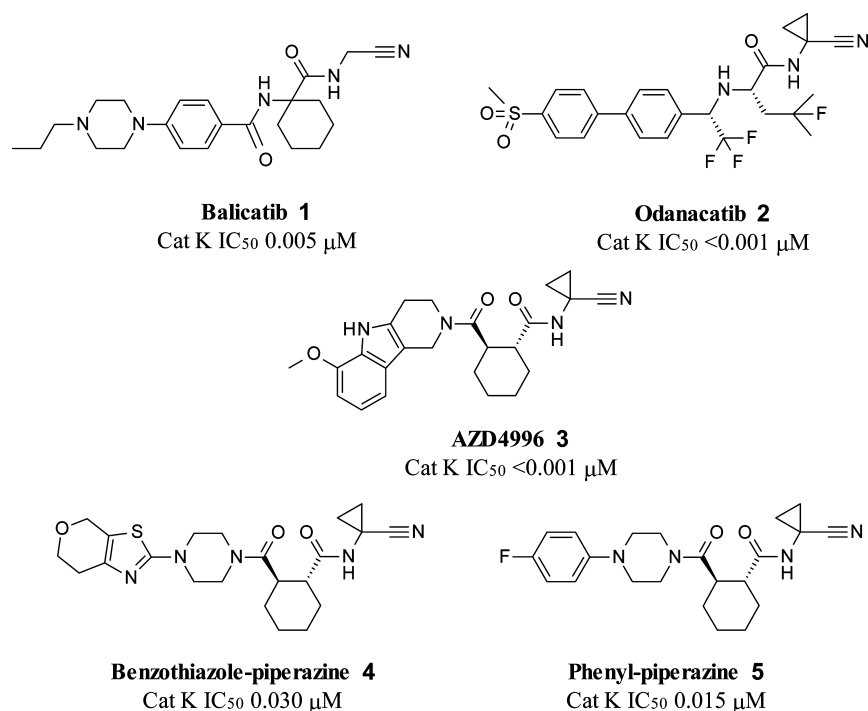


Figure 1. Examples of cathepsin K inhibitors disclosed in the literature, 1–3, plus program start point 5.

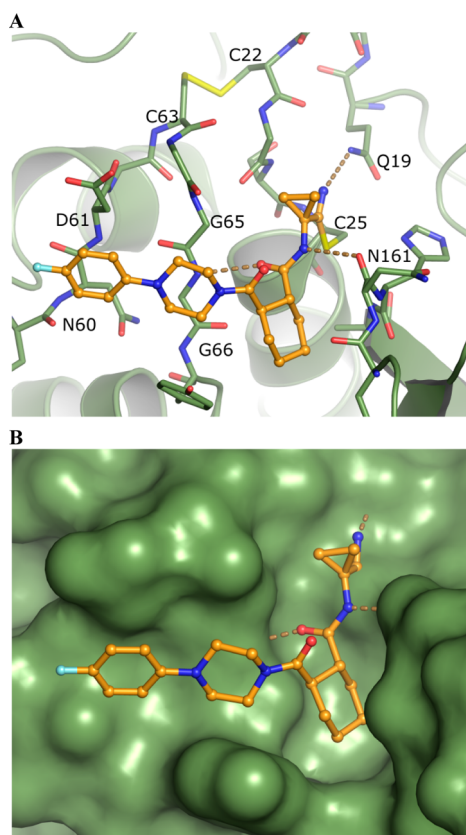


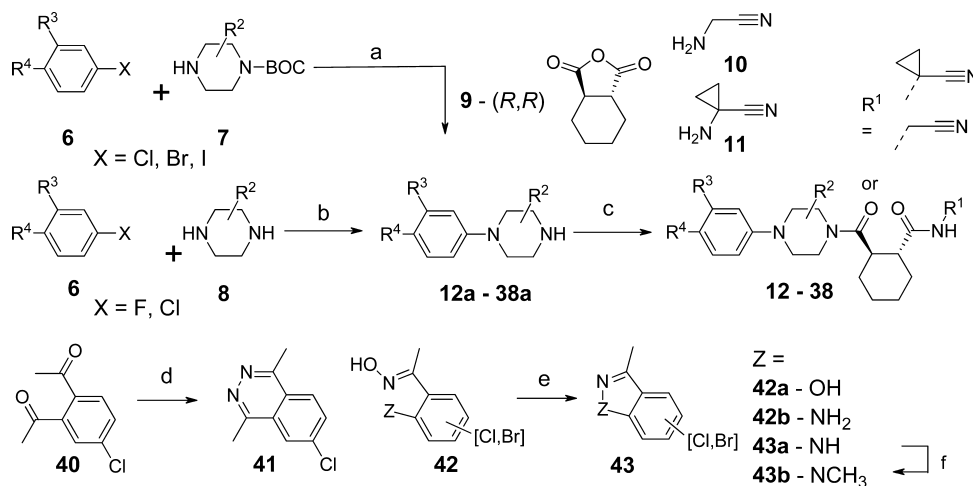
Figure 2. Compound 5 bound to cathepsin K (PDB 4DMX): (A) identification of key H-bonding residues, (B) surface of protein to illustrate the fit of the cyclohexyl and phenylpiperazine moieties.

occupied the P3 region (known as the glycine shelf, Tyr67–Gly66–Gly65) of the protein. Compound 5 was a potent starting point, with good LE (0.37) and ligand-lipophilicity

efficiency ($LLE = pIC_{50} - \log D_{7.4} = 5.7$), but lacked oral bioavailability in rat ($F = 0\%$, clearance (Cl) 36 ± 9.2 mL/min/kg, volume of distribution (V_{dss}) 1.3 ± 1.6 L/kg). Previously we found that changing the group occupying the P3 groove (in this case, phenylpiperazine) of our inhibitors improved the physical and pharmacokinetic properties without resorting to changing the cyclohexyl bisamide, so we focused our efforts on this group. Cognizant of the potential for lysosomotropism and phospholipidosis with basic compounds, we aimed to keep the inhibitors neutral.^{21–24} As a result, and reasoning that with neutral compounds the volume of distribution might be expected to be around 1 L/kg (1.3 L/kg in 5), we were acutely aware that low levels of metabolic clearance would be required to achieve properties consistent with the possibility of once-daily dosing schedules. Increased inhibition of the Cat K enzyme would also reduce the dose level, and having achieved <1.0 nM with carboline 3, we sought to increase potency (aiming for at least single-digit nanomolar). With this in mind, we started our efforts with goals of increasing Cat K potency (<10 nM), improving bioavailability (>40% in rodent), and driving metabolism down to a minimum (HLM < 2.0 μ L/min/mg), by investigating the structure–activity relationships (SARs) around the phenyl and piperazine groups.

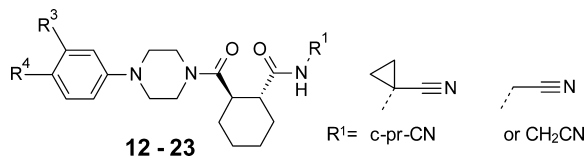
CHEMISTRY

Phenylpiperazines were synthesized in one of two general methods, either leaving group displacement from a substituted aryl (6) or employing palladium coupling conditions with piperazines, either carbamate-protected (7) or unprotected (8) (Scheme 1). Although diversity was introduced early, the route was short and convenient, and the use of protecting groups allowed the location of group R^2 as required. We found the palladium complex [1,3-bis(2,6-diisopropylphenyl)imidazol-2-ylidene](3-chloropyridyl)palladium(II) dichloride (PEPPSI) to be an excellent catalyst for the Buchwald–Hartwig couplings.²⁵ Most notably at the time, good yields could be obtained using

Scheme 1. Synthesis of Cyclohexyl-1,2-diamides 4–38^a

^aReagents and conditions: (a) (i) K_2CO_3 (5 equiv), DMF, 100 °C, 5 h, 23–49%, or (ii) PEPPSI (10 mol %), $KOtBu$ (2 equiv), DME, 70 °C, 18 h; then (iii) 5 equiv of 1.0 M HCl in dioxane, rt, 1 h, or TFA, CH_2Cl_2 , overall 15–52% yield; (b) (i) K_2CO_3 (5 equiv), DMF, 100 °C, 5 h, 45–89%, or (ii) $Pd(OAc)_2$ (10 mol %), BINAP (10 mol %), $NaOtBu$ (2 equiv), toluene, 90 °C, 18 h, overall 25–68% yield; (c) (i) (R,R)-9, CH_2Cl_2 or DMF, rt, 1 h; (ii) CH_2Cl_2 or DMF, DIPEA (5 equiv), HATU (1.1 equiv), **11** or **10** (1.0 equiv), rt, 12 h, 8–84% yield; (d) $NH_2NH_2 \cdot H_2O$, EtOH, rt, 18 h, 92%; (e) Ac_2O neat, 10–60 min, 60–83%; (f) CH_3I (2 equiv), K_2CO_3 , DMF, rt, 5 h, 61–85%.

Table 1. SAR of Phenylpiperazine Compounds



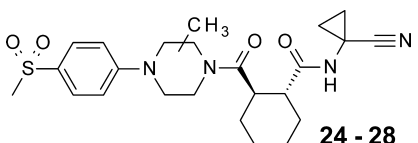
compd	R ⁴	R ³	nitrile R ¹	Cat K IC ₅₀ ^a (μM)	Cat S IC ₅₀ ^a (μM)	Cat B IC ₅₀ ^a (μM)	log $D_{7.4}$ ^c	LE ^d	hPPB ^e (% free)	aqueous solubility (μM), pH 7.4	HLM ^e ($\mu L/min/mg$)	RLM ^f ($\mu L/min/mg$)
12	H	H	CH ₂ CN	0.007	1.03	0.455	1.8	0.43	>50	640	7.7	115
13	F	H	CH ₂ CN	0.023	1.68	0.315	1.9	0.39	39	>3700	<2.9	31
14	CH ₃	H	CH ₂ CN	0.011 ^b		0.572 ^b		0.42				
15	OCH ₃	H	CH ₂ CN	0.006	1.05	0.399	1.6	0.40	>50	390	7.1	77
16	H	OCH ₃	CH ₂ CN	0.008				0.39			5.6	149
17	OCH ₃	OCH ₃	CH ₂ CN	0.006	1.09	1.27		0.37			2.2	6.8
18	CN	H	CH ₂ CN	0.025	2.6		1.8	0.37	53	140		
19	SO ₂ CH ₃	H	CH ₂ CN	0.011	1.29	1.18	0.67	0.36	>50	280	<2.0	<5.3
20	H	H	c-pr-CN	0.015	2.26	1.44	2	0.38	>28	2700	6.9	107
5	F	H	c-pr-CN	0.015	1.31	1.09	2.1	0.37	>50	>4300	<6.3	35
21	OCH ₃	H	c-pr-CN	0.014	2.95	1.44	1.7	0.36	46	>2000	<2.0	48
22	OCH ₃	OCH ₃	c-pr-CN	0.009	2.29	3.06	1.4	0.34	45	>2500	2.3	<7.4
23	SO ₂ CH ₃	H	c-pr-CN	0.018	2.15	2.4		0.33	>50	2500	<2.0	<2.2

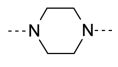
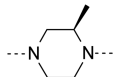
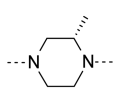
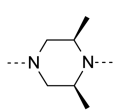
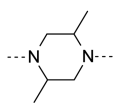
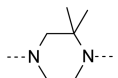
^aBinding affinity for cathepsin versus FRET substrate, mean of greater than $n = 4$ tests, unless otherwise stated. All compounds test at $>10 \mu M$ for Cat L. ^bMean of $n = 2$ tests. ^cStandard methods were used to determine log $D_{7.4}$ and protein binding.³⁹ ^dUnits of $kJ mol^{-1} Da^{-1}$. ^eIn vitro human liver microsomal turnover mean of at least $n = 2$ tests ($\mu L/min/mg$), unless otherwise stated. ^fIn vitro rat liver microsomal turnover mean of at least $n = 2$ tests ($\mu L/min/mg$).

aryl chlorides. Nucleophilic aromatic substitution of a fluoro or chloro group on phenyl **6**, where R³ or R⁴ was an electron-withdrawing group, was high yielding but required elevated temperatures. Following either route, simple deprotection with acid yielded the arylpiperazines **12a–38a** ready for coupling. Ring-opening of chiral anhydride (R,R)-**9** with the piperazines **12a–38a** gave an intermediate acid, which taken forward in one pot gave final compounds **12–38** by amide formation with 1,1-aminocyclopropyl nitrile **10** or **11** and a suitable coupling reagent, such as *O*-(7-azabenzotriazol-1-yl)-*N,N,N',N'*-tetramethyluronium hexafluorophosphate (HATU) and diisopropyle-

thylamine (DIPEA) in yields of up to 84%.²⁶ Bicyclic heteroaromatic halides were synthesized by known literature methods. In short, condensation of diacetylchlorobenzene (**40**) with hydrazine formed **41**; ring closure of hydroxy imines **42** using acetic anhydride to form a leaving group gave the required pyrazolo and isoxazolo bicycles **43**. Finally, in the case of **43a**, the ring nitrogen could be alkylated with methyl iodide under basic conditions to yield **43b**. Isomeric pyrazoles could be generated by varying the starting benzyl halide.

Table 2. SAR for Piperazine Substitution



Compd	Piperazine	Cat K IC50 ^a (μM)	Cat S IC50 ^a (μM)	Cat B IC50 ^a (μM)	LE ^c	HLM $\mu\text{L}/\text{min}/\text{mg}^{\text{d}}$	RLM $\mu\text{L}/\text{min}/\text{mg}^{\text{e}}$
23		0.018	2.15	2.4	0.33	<2.0	<2.2
24		0.012	0.549	0.977	0.33	9.4	<2.0
25		0.059	1.51	3.43	0.30	<2.0	<2.0
26		0.211 ^b	>11.8 ^b	24.9 ^b	0.27	<2.0	<2.0
27		0.312 ^b	>7.43 ^b	40 ^b	0.26	<2.0	4.3
28		0.045	3.75	3.51	0.30	<2.0	4.9

^aBinding affinity for cathepsin versus FRET substrate, mean of greater than $n = 4$ tests, unless otherwise stated. All compounds test at $>10 \mu\text{M}$ for Cat L. ^bMean of $n = 2$ tests. ^cUnits of $\text{kJ mol}^{-1} \text{Da}^{-1}$. ^dIn vitro human liver microsomal turnover mean of at least $n = 2$ tests ($\mu\text{L}/\text{min}/\text{mg}$), unless otherwise stated. ^eIn vitro rat liver microsomal turnover mean of at least $n = 2$ tests ($\mu\text{L}/\text{min}/\text{mg}$).

RESULTS AND DISCUSSION

A small, focused library was prepared to investigate the effect of substitution on the aryl group and two different electrophilic nitrile groups (Table 1). These showed that substitution around the aryl ring was well tolerated with respect to Cat K potency, as well as both methylene (12–19) and cyclopropyl (5, 20–23) groups adjacent to the nitrile. Of these, the cyclopropyl seemed to offer a modest improvement in aqueous solubility (e.g., matched pair 12 and 20), metabolic stability (15 versus 21), and modest Cat B selectivity over Cat K (e.g., 17, 211-fold, and 22, 340-fold). Unfortunately, despite exhibiting good metabolic stability in human liver microsomes, poor rat pharmacokinetic profiles were still observed (e.g., 20, $F = 0.2\%$, $\text{Cl} = 19 \text{ mL}/\text{min}/\text{kg}$; 21, $F = 3.5\%$, $\text{Cl} > 73 \text{ mL}/\text{min}/\text{kg}$; both $n = 1$ experiments, Table 5). A standout from our initial investigations was the somewhat unexpected and synergistic effect of disubstitution at the 3,4-positions of the aryl group. Specifically, by comparing piperazines 15 with 17, and 21 with 22, we observed that methoxy groups at both the 3- and 4-positions of the phenyl ring resulted in compounds with greater resistance toward metabolism in both human and rat liver microsomes. In the case of 22, enzyme affinity was maintained, and when profiled, improved oral bioavailability in rat was observed (41% for 22 vs 3.5% for 21 and 0.2% for 20). This improvement in metabolic stability was initially surprising, given that the addition of methoxy groups represents the introduction of additional potential sites of metabolism. Consistent with this observation, improved HLM stability

following the introduction of 1,2- $(\text{CH}_3\text{O})_2$ onto a phenyl group has also been reported in two large matched pair studies.^{27,28} A similar synergistic effect of 1,2- $(\text{OCH}_3)_2$ substitution with other rigid secondary amides was also observed in other Cat K inhibitor series we have explored (see Table S1 in the Supporting Information). Additionally, the introduction of a sulfone group showed significant promise. In comparing 19 and 23, the cyclopropyl nitrile-containing example had increased solubility by nearly 10-fold. In 19, the sulfone reduced lipophilicity ($\log D_{7.4} = 0.67$) relative to the unsubstituted phenyl 12; however, its solubility decreased. We suggest that the introduction of a sulfone may have increased crystal packing, as recently reported for a series of GPR 119 agonists.²⁹ In addition, both 19 and 23 had markedly improved metabolic stability, with the result that when 23 was studied in vivo, bioavailability improved to 16% (rat in vivo $\text{Cl} = 22 \text{ mL}/\text{min}/\text{kg}$). As a result of these interesting observations, further analogues to investigate the SAR around the dimethoxy and sulfone moieties were studied.

In efforts to maximize enzyme affinity, we explored substitution of the piperazine ring with the aim of making beneficial hydrophobic contacts with the glycine shelf (Table 2). It was hoped that, in compounds such as 24, where the (R)-methyl group adopts an axial position adjacent to the amide, that an increase in binding affinity would be observed due to contact with Tyr67. 24 proved to be similar to 23 in Cat K inhibition, with small erosions in selectivity and HLM stability (9.4 versus $<2.0 \mu\text{L}/\text{min}/\text{mg}$ for 23). A reduction in affinity and LE was obtained with the rest of the substituted

Table 3. In Vitro Biological and Physical Properties of Substituted Aryl-(*R*)-2-methylpiperazines

12, 22, 24, 29 - 31 R¹ = c-pr-CN or CH₂CN

compd	R ⁴	R ³	R ²	R ¹	Cat K IC ₅₀ ^a (μ M)	Cat S IC ₅₀ ^a (μ M)	Cat B IC ₅₀ ^a (μ M)	log <i>D</i> _{7.4}	LE ^c	HLM ^d (μ L/min/mg)	RLM ^e (μ L/min/mg)
12	H	H	H	c-pr-CN	0.007	1.03	0.455	1.8	0.43	7.7	115
22	OCH ₃	OCH ₃	H	c-pr-CN	0.009	2.29	3.06	1.4	0.34	2.3 \pm 0.7	7.4
24	SO ₂ CH ₃	H	CH ₃	c-pr-CN	0.012	0.549	0.977		0.33	9.4	<2.0
29	H	H	CH ₃	c-pr-CN	0.011 ^b	1.30 ^b	0.649 ^b	2.4	0.38	20	>347
30	H	H	CH ₃	CH ₂ CN	0.006 ^b	1.22 ^b	0.462 ^b		0.42	16	>347
31	OCH ₃	OCH ₃	CH ₃	c-pr-CN	0.004	1.45	1.85	1.9	0.35	<2.0 (<i>n</i> = 6)	5.1

^aBinding affinity for cathepsin versus FRET substrate, mean of greater than *n* = 4 tests, unless otherwise stated. All compounds test at >10 μ M for Cat L. ^bMean of *n* = 2 tests. ^cUnits of $\text{kJ mol}^{-1} \text{Da}^{-1}$. ^dIn vitro human liver microsomal turnover mean of at least *n* = 2 tests (μ L/min/mg), unless otherwise stated. ^eIn vitro rat liver microsomal turnover mean of at least *n* = 2 tests (μ L/min/mg).

piperazines when combined with the 4-CH₃SO₂Ph group (**25–28**), although the in vitro metabolic stability was retained. In summary, sulfone **23** appeared the best compound from this series. When explored in rat PK, **23** also had improved bioavailability (*F* = 16%).

In contrast, when the substituted piperazine was combined with the 3,4-(CH₃O)₂Ph group, a significant improvement was observed (Table 3). Compared with **12**, the (*R*)-methyl offered no improvement in potency or metabolic stability when combined with either nitrile headgroup (**29**, **30**). However, dimethoxy compound **31** gave a small increase in potency and reached the limit of quantification for our standard HLM assay. To quantify the stability of the compound, **31** was subjected, at 1.0 μ M concentration, to a prolonged incubation period (120 min) with HLM in the absence of albumin. This gave a measured turnover of 0.7 μ L/min/kg, demonstrating that **31** has excellent metabolic stability. Repeat testing of Cat K inhibition for **12** and **31** yielded a mean IC₅₀ of 8.9 \pm 3.0 nM (*n* = 6) and 4.1 \pm 0.9 nM (*n* = 10), respectively, proving that the small activity difference was real. We postulate that this was caused, at least in part, by a conformational lock, which has occurred as a result of the addition of the (*R*)-methyl group on the piperazine. This could result in an optimized entropic *minimum*, positioning one methoxy group for improved surface contact. Equally, with such a small change as this, the result could be a simple hydrophobic effect. Figure 3 shows a matched pair analysis across all the piperazine/(*R*)-2-methylpiperazines prepared in the program, demonstrating this effect was consistent.³⁰ The opposite (*S*)-methyl enantiomer had considerably reduced binding affinity (0.087 μ M at Cat K, not shown). Overall, the small increase in activity of the combination of 3,4-(CH₃O)₂Ph and (*R*)-2-methylpiperazine, in addition to metabolic stability improvements, meant that the 3,4-(CH₃O)₂Ph series showed greater promise than the sulfones (compare **24** and **31**).

When dosed to rats, **31** also had good oral exposure and a profile similar to that of the the desmethylpiperazine **22** (*F* = 46% vs 41%, *Cl* = 21 versus 29 mL/min/kg). Moving to higher species, both **22** and **31** had high bioavailability (*F* = 79% and 71%) and low to moderate clearance (12.0 and 8.6 mL/min/kg, respectively) in dog. The 3,4-(CH₃O)₂Ph group also caused a reduction in lipophilicity (mean Δ log *D*_{7.4} = -0.45; compare **12** to **22** and **29** to **31**), and the free fraction in human plasma was also good (**22** and **31** hu = 45% and 39% free, respectively).

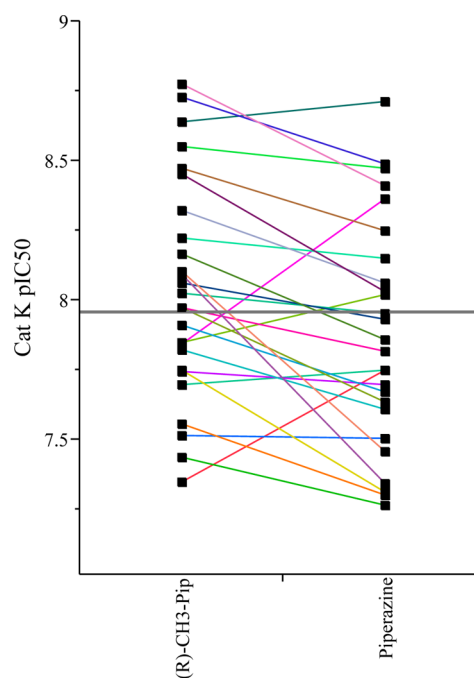
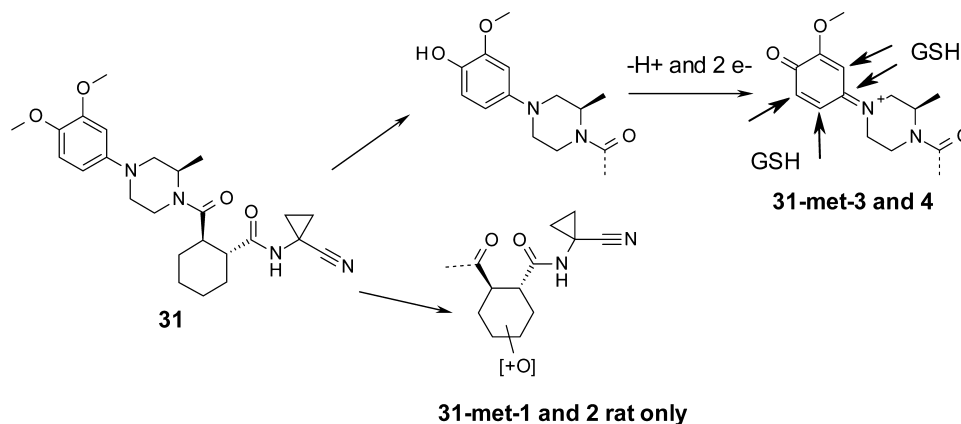


Figure 3. Cat K inhibition for matched pairs of piperazine versus (*R*)-2-methylpiperazine. Improvement in mean Δ pIC₅₀(Cat K) = 0.15 \pm 0.08, *p* < 0.05, and *n* = 27. Colored lines indicate matched pairs.

Both compounds were active in a low-throughput primary human cell osteoclast “pit” resorption assay at potencies of IC₅₀ = 0.126 and 0.040 μ M, respectively (both *n* = 1). This technically demanding assay measured the ability of compounds to stop the osteoclast cells dissolving cartilage and bone, thereby stopping the observed formation of pits in the bone sample (see the Supporting Information). Results were only considered qualitatively, as no relationship was found to pharmacodynamic (PD) end points (data not shown). This compared well with our recently reported Cat K inhibitor AZD-4996 (0.032 \pm 0.007 μ M, *n* = 3) as well as balicatib (0.0266 \pm 0.001 μ M, *n* = 2) and odanacatib (0.100 μ M, *n* = 1), tested in our hands. Overall, in compound **31** we had achieved the desired high affinity, metabolic stability, and in vivo pharmacokinetic (PK) properties for confident scaled prediction to man.

Scheme 2. Metabolites Found after in Vitro Incubation of 31 with Rat and Human Hepatocytes^a

^aSee the Supporting Information for mass spectrometry chromatograms.

Unfortunately, in vitro metabolite identification (MetID) studies showed formation of glutathione (GSH) adducts after incubation in both rat and human hepatocytes. This indicated that reactive metabolites were generated, despite the low metabolic turnover (Scheme 2). In other compounds within this chemical series, MetID had identified the cyclohexyl ring as the primary site of metabolism (Scheme 2, **31-met-1 and 2**). Following demethylation at the 4-OCH₃ group, a second oxidation step may occur to produce an electrophile of a type known to be capable of reacting with GSH (**31-met-3 and 4**).³¹ This electrophilic species can react with GSH at four ring positions to yield glutathione adducts.^{32,33} Several studies have been carried out to measure and quantify the risk posed by reactive metabolites; however, elimination, or at least minimization, is always desirable.³⁴ The benzo[*d*][1,3]dioxol-5-yl compound **32**, which would test the effects of the dimethoxy groups on potency in synergy to the (*R*)-2-methylpiperazine, was prepared. When compared to **31**, **32** was a less potent inhibitor of Cat K and also confirmed what we suspected, i.e., that the dimethoxy groups actually imparted in vitro microsomal stability (both HLM and RLM turnovers were higher, Table 4). As a consequence, we set out to design isosteres with a view to mimicking the observed effect of the 3,4-(CH₃O)₂Ph on PK properties (stability and good bioavailability) and eliminating the formation of reactive metabolites.

Our efforts to address the formation of this putatively reactive metabolite consisted of three main approaches, namely, (i) replacing the 4-OCH₃ with a steric mimic, (ii) making the aryl ring heteroaromatic in attempts to block ring oxidation and subsequent GSH reactivity, and (iii) heterocyclic mimics of the 3,4-(CH₃O)₂Ph motif. The conformation of the 3,4-(CH₃O)₂Ph unit was explored using the Cambridge Structural Database (CSD), and it was found that the bulk of the structures (>95%) were in fact near planar, with CH₃ groups pointing away from each other such that the oxygen lone pairs are oriented toward each other (Figure 4). Modeling studies indicated that a structural change from 4-OCH₃ to 4-cyclopropyl (such as in **33**) might yield compounds of similar shape (Figure 4, structure of **33** overlaid in red), removing the most likely metabolically vulnerable group. In the second approach, it was thought that changing the phenyl ring to a pyridyl should reduce the ability of the methoxy oxygens to

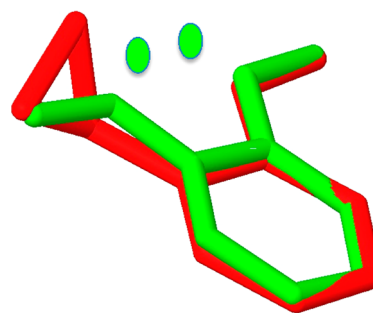


Figure 4. Structure of 3,4-(CH₃O)₂Ph (as in **31**) in green. The CSD searches were for moieties with methyl groups 180° (τ) apart in the same plane. Greater than 95% of the structures found ($n = 1130$) had $\tau > 160^\circ$. This would place the nonbonding lone pairs of electrons of the oxygen atoms toward each other. Electrostatic potential minimum (green spheres, V_{\min}) calculations using this information predicted a $\Delta \log P$ of 0.53, which was consistent with experimental observation in this study (see the Supporting Information, Tables S2 and S3). The 4-cyclopropyl-3-methoxyphenyl moiety is overlaid in red (as in **33**, Table 4). The structure was calculated at the B3LYP/6-31G* level of theory,^{40,41} indicating that this group was a good spatial mimic of the dimethoxy moiety.

stabilize a radical oxidative mechanism. With this in mind, we designed **34**.³⁵

For the third approach we considered replacing the 3,4-(CH₃O)₂Ph group with a bicycle dimethyl heteroaryl group.³² To reduce the synthetic effort required, we studied the electrostatic potential minima (V_{\min}) of the heterocycle isosteres of 3,4-(CH₃O)₂Ph we envisaged via quantum mechanical calculations³⁶ (see the Supporting Information). The two minima for the 3,4-(CH₃O)₂Ph unit (where the oxygen lone pairs are directed toward each other, *vide supra*) were found to be in close proximity, indicating the possibility of replacement by a single minimum (such as the aza group of a heterocycle). Furthermore, these calculations served to explain the observed reduction in lipophilicity resulting from the pair of adjacent methoxy groups.³⁷ Of the bicycles available, phthalazine, benzisoxazole, and indazole looked to be the most attractive, so **35–38** were synthesized (the magnitude of the minimum on a nitrogen lone pair from an indazole, **37**, was similar to that of **31**).

Table 4 summarizes the results of testing analogues **32–37**. When tested, the 4-cyclopropyl compound **33** maintained high

Table 4. Data for Dimethoxy Compound 31 and Isosteres Thereof, 32–38

31 - 38

Compd	R	Cat K IC ₅₀ ^a (μ M)	Cat S IC ₅₀ ^a (μ M)	Cat B IC ₅₀ ^a (μ M)	log $D_{7.4}$	LE ^c	aqueous solubility pH 7.4 (μ M)	HLM μ L/min/mg ^d	RLM μ L/min/mg ^e
31		0.004	1.45	1.85	1.9	0.35	>2400	<2.0 ($n = 6$)	5.1
32		0.009	1.15	0.645	-	0.33	-	8.8	83
33		0.003	1.37	1.14	3.5	0.34	200	9.0	33
34		0.005	1.1	1.69	2.3	0.34	>1700	4.2	13
35		0.017 ^b	1.75 ^b	2.94 ^b	1.9	0.30	-	<2.0	-
36		0.016	0.807	0.603	2.7	0.32	600	9.3	-
37		0.008	1.25	0.766	2.7	0.33	>1100	8.8	15
38		0.009	1.23	0.971	2.8	0.32	>1400	<2.0 ($n = 7$)	4.7

^aBinding affinity for cathepsin versus FRET substrate, mean of greater than $n = 4$ tests, unless otherwise stated. All compounds test at $>10 \mu\text{M}$ for Cat L. ^bMean of $n = 2$ tests. ^cUnits of $\text{kJ mol}^{-1} \text{Da}^{-1}$. ^dIn vitro human liver microsomal turnover mean of at least $n = 2$ tests ($\mu\text{L}/\text{min}/\text{mg}$), unless otherwise stated. ^eIn vitro rat liver microsomal turnover mean of at least $n = 2$ tests ($\mu\text{L}/\text{min}/\text{mg}$).

Cat K potency but did not have the same in vitro stability to HLM. Unfortunately, and perhaps as a consequence of its increased lipophilicity ($\log D_{7.4} = 3.5$), weak CYP3A4 inhibition ($1.6 \mu\text{M}$) was observed for this analogue, and glutathione adducts were still found following incubation with human and rat hepatocytes, ruling out 33 as a viable candidate. 34 represented our second approach, i.e., to change the substituted phenyl into a heterocycle to reduce the formation GSH adducts. As for 33, good Cat K inhibition was maintained, along with a small loss of stability to HLM. Cat K potency and in vitro metabolism were also good for the heterocyclic replacements 35–38, with the benzopyrazoles having 2-fold greater affinity than the other isosteres. Some erosion of selectivity for other cathepsins as well as HLM stability was

observed, which was important for the final compound selection. As such, 38 was the standout compound with good HLM stability maintained below the limit of quantification for the assay.

All the dimethoxy isosteres were progressed to rat PK studies (Table 5). The 4-cyclopropyl (33) and pyridine (34) analogues retained the good bioavailability of 31. Despite good HLM stability, benzopyridazine 35 suffered from high Cl in rat, which appeared to be due, at least in part, to higher turnover in rat hepatocytes. Benzisoxazole 36 had moderate levels of bioavailability and clearance in rat, but the instability in in vitro human hepatocytes meant this projected into high clearance for this example when scaled. In contrast, both indazoles were found to have excellent profiles in rat with high

Table 5. Serum Protein Binding and Selected Pharmacokinetic Data for Dimethoxy 31 and Isosteres

compd	species	protein binding ^a (% free)	in vitro hepatocyte Clint ^b ($\mu\text{L}/\text{min}/10^6$ cells)	Clp (mL/min/kg)	V _{dss} (L/kg)	bioavailability (%)
5	rat ^c	>53	35 (<i>n</i> = 1)	36 ± 9.2	1.3 ± 1.6	0
20	rat ^c	28	36 (<i>n</i> = 1)	19 ^e	1.1 ^e	0.2 ^e
21	rat ^c	25	42 (<i>n</i> = 1)	>73 ^e	1.1 ^e	3.5 ^e
31	rat ^c	53	<2.0 (<i>n</i> = 3)	21 ± 6.1	1.2 ± 0.6	46 ± 23
	dog ^d	39	5.2 (<i>n</i> = 1)	8.7 ± 1.0	0.8 ± 0.3	71 ± 22
	human	39	<2.0 (<i>n</i> = 2)			
33	rat ^c	7.2	13 ± 8.6	39 ^e	2.8	57 ^e
	human	8.1	25 ± 4.0			
34	rat ^c	41	<2.0 (<i>n</i> = 2)	15 ^e	0.7	55 ^e
	human	24				
35	rat ^c	62	12 ± 4.0	>73 ^e	4.1	1.4 ^e
	human	49	<3.0 (<i>n</i> = 2)			
36	rat ^c	14	9.4 ± 2.5	29 ^e	2.1	21 ^e
	human	20	30 ± 4.2			
37	rat ^c	30	4.6 (<i>n</i> = 1)	19 ± 7.8	2.5 ± 0.7	87 ± 15
	human	28	4.7 ± 3.1			
38	rat ^c	27	<2.0 (<i>n</i> = 3)	9.5 ± 5.3	2.5 ± 0.3	64 ± 17
	human	25	<3.0 (<i>n</i> = 2)			

^aAll results are a mean of at least *n* = 2 experiments. Standard methods were used to determine protein binding.³⁹ ^bThe standard deviation is shown where possible. The number of repeat experiments where the result was below the limit of detection is shown in parentheses. All pharmacokinetic experiments are reported as single-dosed compounds in at least two experiments involving two animals in each. ^cAlderley Park Han Wistar male rats, dosed to fed animals, po 2.0 mg/kg as a suspension in 5% DMSO/95% HPMC/TWEEN, iv dosed as a solution in 40% DMA/water at 2.0 mg/kg. ^dBeagle dog, dosed to fasted animals, po 1.0 mg/kg as a suspension in 5% DMSO/95% HPMC/TWEEN, iv dosed as a solution in 10% DMSO/90% Sorensens at 1.0 mg/kg. ^eSingle experiment, mean of two animals.

bioavailability and low clearance, exhibiting profiles reminiscent of the 3,4-(CH₃O)₂Ph 31. The low clearance was explained at least in part by relatively good stability of 37 and 38 in rat microsomes and hepatocytes. Figure 5 shows a head-to-head

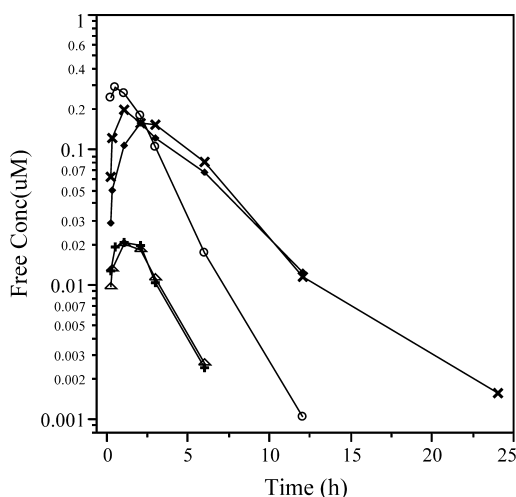


Figure 5. Comparative rat oral pharmacokinetic profiles for selected compounds, adjusted for protein binding: ○, free [31]; +, free [33]; △, free [36]; ●, free [37]; ×, free [38]. Alderley Park Han Wistar male rat, dosed to fed animals, po 2.0 mg/kg as a suspension in 5% DMSO/95% HPMC/TWEEN, single-dosed compounds in at least two experiments involving two animals in each study.

comparison of rat oral pharmacokinetic profiles, adjusted for protein binding, for 31, 33, and 36–38. Most notably, indazole 38 showed an improvement with a sustained higher blood level than the 3,4-(CH₃O)₂Ph lead 31. Overall, while 38 was slightly less potent (approximately 2-fold) than 31, it maintained the other excellent druglike properties, such as good rat PK,

excellent solubility, and cathepsin selectivity (greater than 100-fold over cathepsins L, S, and B). Perhaps most importantly, GSH adducts were not observed following incubation with human and rat hepatocytes in vitro for both 37 and 38.

In summary, we have identified novel cathepsin K inhibitors that show excellent pharmacokinetic profiles. Compounds with the 3,4-(CH₃O)₂Ph motif were identified, most notably 31, and were found to have unexpectedly advantageous PK properties. Metabolite identification studies subsequently identified a reactive metabolite risk with this motif, and structure-based design of isosteres has yielded compounds maintaining many of the good properties. Consistent with our design hypothesis, indazoles 37 and 38 exhibited desirable profiles and appear to have removed the propensity of these compounds to form glutathione-reactive metabolites. Of the two indazoles, 38 was selected as the compound with the most balanced profile to be progressed into further studies, which will be reported in due course.

EXPERIMENTAL SECTION

All solvents and chemical used were reagent grade. Anhydrous solvents tetrahydrofuran (THF) and dimethoxyethane (DME) were purchased from Aldrich. Purity and characterization of the compounds were established by a combination of low-resolution mass spectrometry (LC-MS) (Waters liquid chromatography-mass spectrometry system), where purity was determined by UV absorption (254 nm) and the mass ion was determined by electrospray ionization (Micromass instrument), and NMR analytical techniques. All test compounds were >95% pure. ¹H NMR spectra were recorded using a Varian AV400 FT spectrometer or via the flow NMR process using an Avance 500 FT spectrometer, and using DMSO-*d*₆ or CDCl₃ with the data expressed as chemical shifts (ppm) from internal standard TMS on the δ scale. Splitting patterns are indicated as follows: s, singlet; d, doublet; t, triplet; m, multiplet; br, broad peak. Compound 38 when measured by ¹H NMR at ambient temperature showed differential rotameric peaks around the tertiary amide group. In these cases assignments for protons, which were measured distinctly, have been

expressed as fractions (e.g., 0.5H). The reversed-phase column used was a 4.6 mm × 50 mm Phenomenex Synergi Max-RP 80 Å, and the solvent system was water containing 0.1% formic acid and acetonitrile unless otherwise stated. A typical run was 5.5 min with a 4.0 min gradient from 0% to 95% acetonitrile. Purification by column chromatography was typically performed using silica gel (Merck 7734 grade), and solvent mixtures and gradients are recorded herein. Purification by reversed-phase high-performance chromatography was typically performed using a Perkin-Elmer instrument using UV detection at 254 nm and a C18 1500 × 21.2 mm Phenomenex column, 100 Å. Acidic conditions (0.1–0.5% formic acid) or basic conditions (ammonia to pH 10) were used with gradient solvent mixtures of acetonitrile and water. Strong cation exchange (SCX) columns were supplied from International Sorbent Technology.

General Procedure for the Preparation of 22, 24, 31, and 38.

An appropriate amine (1.0 equiv) was added to (3aR,7aR)-hexahydroisobenzofuran-1,3-dione (**9**; 1.0 equiv) and DIPEA (3.0 equiv) in CH₂Cl₂ to a concentration of 0.1 M. The resulting solution was stirred at 20 °C for 18 h, and then either aminoacetonitrile hydrochloride (**10**) or **11** (3.0 equiv) was added followed by HATU (1.1 equiv) and further DIPEA (5.0 equiv). The resulting suspension was stirred at 20 °C for 72 h. The solution was diluted with CH₂Cl₂ (equal volume), partitioned with 50% brine (equal volume), then dried (Na₂SO₄), concentrated in vacuo, and adsorbed onto silica. Flash chromatography (silica, 0–100% EtOAc in isohexane) yielded the desired compound usually as a solid or alternative by preparative HPLC where stated.

(1R,2R)-2-[[4-(3,4-Dimethoxyphenyl)piperazin-1-yl]carbonyl]cyclohexanecarboxylic Acid (1-Cyanocyclopropyl)amide (22). **9** (1.00 g, 5.81 mmol) and 1-(3,4-dimethoxyphenyl)piperazine (1.10 g, 6.10 mmol), combined with **11** (0.82 g, 6.97 mmol), HATU (3.10 g, 8.13 mmol), and DIPEA (3.00 mL, 17.4 mmol) in DMF (20 mL), yielded **22** (193 mg, 58%) as a white foam: ¹H NMR (400 MHz, CDCl₃) δ 1.08–1.20 (m, 2H), 1.24–1.65 (m, 6H), 1.55–1.90 (m, 4H), 2.58 (td, *J* = 10.5, 3.5 Hz, 1H), 2.78 (td, *J* = 12.3, 3.5 Hz, 1H), 3.02–3.07 (m, 3H), 3.14–3.19 (m, 1H), 3.60–3.70 (m, 2H), 3.83 (s, 3H), 3.86 (s, 3H), 3.70–3.92 (m, 2H), 6.46 (dd, *J* = 8.6, 2.7 Hz, 1H), 6.57 (d, *J* = 2.7 Hz, 1H), 6.59 (s, 1H), 6.78 (d, *J* = 8.7 Hz, 1H); HRMS (ES+) *m/z* for C₂₄H₃₃O₄N₄ (M⁺ + H), calcd 441.2496, found 441.2498.

(1R,2R)-N-(1-Cyanocyclopropyl)-2-[[4-(4-(methylsulfonyl)phenyl)piperazin-1-yl]carbonyl]cyclohexanecarboxamide (23). **9** (159 mg, 1.04 mmol) was added to 4-[4-(methylsulfonyl)phenyl]piperazine (250 mg, 0.98 mmol) in DCM (3 mL) at room temperature. The resulting solution was stirred at room temperature for 3 days. To the reaction mixture were added HATU (509 mg, 1.20 mmol), **11** (159 g, 1.20 mmol), and DIPEA (0.50 mL, 2.86 mmol). The resulting solution was stirred at room temperature for 16 h to afford **23** as a colorless gum (165 mg, 35% yield): MS (+ve ESI) *m/z* 459 (M + H)⁺; ¹H NMR (400.13 MHz, CDCl₃) δ 1.12–1.20 (m, 2H), 1.32 (d, 1H), 1.36–1.45 (m, 2H), 1.46–1.52 (m, 2H), 1.60 (m, 1H), 1.83–1.85 (m, 4H), 2.51–2.58 (m, 1H), 2.94–3.02 (m, 1H), 2.97–3.01 (s, 3H), 3.14–3.19 (m, 1H), 3.39 (m, 2H), 3.47 (m, 2H), 3.65–3.68 (m, 1H), 3.87–3.98 (m, 2H), 6.76 (s, 1H), 6.91 (m, 2H), 7.76–7.80 (m, 2H).

(R)-tert-Butyl 4-(3,4-dimethoxyphenyl)-2-methylpiperazine-1-carboxylate (39). Palladium(II) acetate (0.052 g, 0.230 mmol) and (R)-(+)-2,2'-bis(diphenylphosphino)-1,1'-binaphthyl (0.115 g, 0.180 mmol) were added to 4-bromoveratrole (0.662 mL, 4.61 mmol), (R)-1-*N*-Boc-2-methylpiperazine (0.923 g, 4.61 mmol), and sodium *tert*-butoxide (0.664 g, 6.91 mmol) in anhydrous toluene (12 mL) under argon. The resulting solution was stirred at reflux for 16 h. The reaction mixture was diluted with Et₂O and filtered through Celite. The resulting mixture was evaporated to dryness to afford crude (R)-*tert*-butyl 4-(3,4-dimethoxyphenyl)-2-methylpiperazine-1-carboxylate. The crude product was purified by flash silica chromatography, elution gradient 0–25% EtOAc in isohexane. Pure fractions were evaporated to dryness to afford **39** (0.871 g, 56%) as a beige solid: MS (+ve ESI) *t_R* = 2.57 min, *m/z* 337.31 (M + H)⁺; ¹H NMR (400.132 MHz, CDCl₃) δ 1.33 (d, 3H), 1.49 (s, 9H), 2.67 (td, *J* = 11.7, 3.4 Hz,

1H), 2.85 (dd, *J* = 11.7, 3.7 Hz, 1H), 3.24 (ddd, *J* = 11.7, 9.5, 2.6 Hz, 2H), 3.36 (d, *J* = 11.5 Hz, 1H), 3.84 (s, 3H), 3.88 (s, 3H), 3.94 (d, *J* = 13.8 Hz, 1H), 4.34 (s, 1H), 6.42 (dd, *J* = 8.6, 2.6 Hz, 1H), 6.53 (d, *J* = 2.6 Hz, 1H), 6.80 (d, *J* = 8.7 Hz, 1H).

(R)-1-(3,4-Dimethoxyphenyl)-3-methylpiperazine Hydrochloride (31a). **39** (0.400 g, 1.19 mmol) was added to hydrochloric acid in methanol (methanol reagent 10) (15 mL, 1.19 mmol), and the resulting solution was stirred at room temperature for 16 h. The resulting mixture was evaporated to dryness, and the residue was azeotroped with CH₂Cl₂ to afford crude **31a** (100%): MS (+ve ESI) *t_R* = 1.22 min, *m/z* 237.30 (M + H)⁺.

(1R,2R)-N-(1-Cyanocyclopropyl)-2-[[4-(3,4-dimethoxyphenyl)-2-methylpiperazin-1-yl]carbonyl]cyclohexanecarboxamide (31). **9** (159 mg, 1.04 mmol) was added to **31a** (338 mg, 1.24 mmol) in DCM (3 mL) at room temperature. The resulting solution was stirred at room temperature for 3 days. To the reaction mixture were added HATU (509 mg, 1.20 mmol), **11** (159 g, 1.20 mmol), and DIPEA (0.50 mL, 2.86 mmol). The resulting solution was stirred at room temperature for 16 h to afford **31** (320 mg, 57%) as a cream solid: ¹H NMR (400.132 MHz, DMSO) δ 0.91–1.47 (m, 12H), 1.64–1.82 (m, 4H), 2.37 (m, 1H), 2.54–2.96 (m, 3H), 3.37–3.54 (m, 2H), 3.68 (s, 3H), 3.75 (s, 3H), 3.91–4.67 (m, 2H), 6.46 (dd, *J* = 8.6, 2.6 Hz, 1H), 6.61 (d, *J* = 8.7, 2.6 Hz, 1H), 6.81 (d, *J* = 8.7 Hz, 1H), 8.69 (br, 1H); HRMS (ES+) *m/z* for C₂₅H₃₅O₄N₄ (M⁺ + H), calcd 455.2653, found 455.2654.

(R)-4-(1,3-Dimethyl-1*H*-indazol-5-yl)-2-methylpiperazine (38a). 5-Bromo-1,3-dimethyl-1*H*-indazole³⁸ (0.448 g, 1.99 mmol) was reacted with (R)-1-*N*-Boc-2-methylpiperazine (0.399 g, 1.99 mmol) to afford **40** (0.363 g, 52.9%) as a white solid after isolation (preparative HPLC) and workup: MS (+ve ESI) *t_R* = 2.58 min, *m/z* 345.55 (M + H)⁺; ¹H NMR (400 MHz, CDCl₃) δ 1.37 (d, *J* = 6.7 Hz, 3H), 1.50 (s, 9H), 2.52 (s, 3H), 2.72 (td, *J* = 11.8, 3.8 Hz, 1H), 2.88 (dd, *J* = 11.8, 3.8 Hz, 1H), 3.29 (ddd, *J* = 16.4, 11.7, 5.0 Hz, 2H), 3.41 (d, *J* = 10.2 Hz, 1H), 3.96–4.01 (m, 4H), 4.37 (s, 1H), 7.00 (d, *J* = 2.0 Hz, 1H), 7.14 (dd, *J* = 9.0, 2.0 Hz, 1H), 7.25 (d, *J* = 9.0 Hz, 3H). **40** (0.363 g, 1.05 mmol) was added to hydrochloric acid in methanol (methanol reagent 10) (15 mL, 1.05 mmol), and the resulting solution was stirred at room temperature for 16 h to afford **38a** (80%) as a yellow gum after workup and isolation: MS (+ve ESI) *t_R* = 1.27 min, 245.50 (M + H)⁺; ¹H NMR (400 MHz, CDCl₃) δ 1.21 (d, *J* = 6.4 Hz, 3H), 2.05 (br, 1H), 2.44 (dd, *J* = 10.3, 10.7 Hz, 1H), 2.53 (s, 3H), 2.78 (td, *J* = 11.4, 3.4 Hz, 1H), 2.91–3.30 (m, 3H), 3.44 (d, *J* = 12.1 Hz, 2H), 3.96 (s, 3H), 7.03 (d, *J* = 1.9 Hz, 1H), 7.18 (dd, *J* = 9.0, 1.9 Hz, 1H), 7.03 (d, *J* = 9.0 Hz, 1H).

(1R,2R)-N-(1-Cyanocyclopropyl)-2-[[4-(1,3-dimethyl-1*H*-indazol-5-yl)-2-methylpiperazin-1-yl]carbonyl]cyclohexanecarboxamide (38). **9** (0.065 g, 0.42 mmol) was added to **38a** (0.103 g, 0.42 mmol) in DCM (3 mL) at room temperature. The resulting solution was stirred at room temperature for 5 h. To the reaction mixture were added HATU (0.224 g, 0.59 mmol), 1-amino-1-cyclopropanecarbonitrile hydrochloride (0.065 g, 0.55 mmol), and DIPEA (0.220 mL, 1.26 mmol). The resulting solution was stirred at room temperature for 3 d to afford **38** (134 mg, 69%) as a cream solid after workup and isolation: ¹H NMR (400.132 MHz, DMSO) δ 0.91–1.08 (m, 2H), 1.12–1.48 (m, 9H), 1.65–1.84 (m, 4H), 2.41 (s, 3H), 2.54 (m, 1H), 2.60–3.00 (m, 3H), 3.38 (m, 1H), 3.40–3.55 (m, 2H), 3.90 (s, 3H), 3.97 (d, *J* = 13.8 Hz, 0.5H), 4.24 (d, *J* = 11.9 Hz, 1.0H), 4.69 (s, 0.5H), 7.04 (m, 1H), 7.20 (dd, *J* = 9.1, 7.2 Hz, 1H), 7.45 (d, *J* = 9.1 Hz, 1H), 8.69 (s, 0.5H), 8.71 (s, 0.5H); HRMS (ES+) *m/z* for C₂₆H₃₅O₂N₆ (M⁺ + H), calcd 463.2816, found 463.2817.

■ ASSOCIATED CONTENT

Supporting Information

Table S1 detailing the data from a series of tetrahydroisoquinoline and isoquinolines with and without 1,2-(OCH₃)₂ groups, procedures for the preparation of **5**, **12–21**, **24–30**, and **32–37**, human and rat in vitro hepatic incubations and metabolite identification studies, procedures for the testing of compounds in cathepsin K, S, L, and B and the osteoclast cell assay, and

CCDB search data for the τ angle between 1,2-(CH₃O)₂-Ph and V_{\min} to $\Delta \log P$ calculations. This material is available free of charge via the Internet at <http://pubs.acs.org>.

AUTHOR INFORMATION

Corresponding Author

*Phone: +44 (0) 7720685539 (A.J.D.); +1 650 467 8886 (J.J.C.). E-mail: aldossetter@gmail.com (A.J.D.); crawford.james@gene.com (J.J.C.).

Present Address

[§]Genentech Inc., 1 DNA Way, South San Francisco, CA 94080.

Author Contributions

^{||}These authors contributed equally to this work.

Notes

The authors declare no competing financial interest.

ABBREVIATIONS USED

PEPPSI, [1,3-bis(2,6-diisopropylphenyl)imidazol-2-ylidene](3-chloropyridyl)palladium(II) dichloride; OA, osteoarthritis; OP, osteoporosis; MBD, metastatic bone disease; Cat K, cathepsin K; Cat S, cathepsin S; Cat B, cathepsin B; Cat L, cathepsin L; HATU, *O*-(7-azabenzotriazol-1-yl)-*N,N,N',N'*-tetramethyluronium hexafluorophosphate; PYBOP, (benzotriazolyl)oxy-tripyrrolidinophosphonium hexafluorophosphate; DIPEA, diisopropylethylamine; LLE, ligand lipophilicity efficiency; Hep, hepatocyte; HLM, human liver microsome; RLM, rat liver microsome; CTX-1, C-telopeptide fragment of type I collagen; QFRET, quenched fluorescent resonance energy transfer technology; CCP4, collaborative computational project, number 4; CSD, Cambridge Structural Database (<http://www.ccdc.cam.ac.uk/products/csd/>); V_{\min} , electrostatic potential minima; Cl, clearance; V_{dss} , volume of distribution

REFERENCES

- (1) Teitelbaum, S. L. Bone resorption by osteoclasts. *Science* **2000**, *289*, 1504–1508.
- (2) Lawrence, R. C.; Felson, D. T.; Helmick, C. G.; Arnold, L. M.; Choi, H.; Deyo, R. A.; Gabriel, S.; Hirsch, R.; Hochberg, M. C.; Hunder, G. G.; Jordan, J. M.; Katz, J. N.; Kremers, H. M.; Wolfe, F.; National Arthritis Data Workgroup. Estimates of the prevalence of arthritis and other rheumatic conditions in the United States. Part II. *Arthritis Rheum.* **2008**, *58*, 26–35.
- (3) Gupta, S.; Singh, R. K.; Dastidar, S.; Ray, A. Cysteine cathepsin S as an immunomodulatory target: present and future trends. *Expert Opin. Ther. Targets* **2008**, *12*, 291–299.
- (4) Stoch, S. A.; Wagner, J. A. Cathepsin K inhibitors: a novel target for osteoporosis therapy. *Clin. Pharmacol. Ther.* **2008**, *83*, 172–176.
- (5) Yasuda, Y.; Kaleta, J.; Broemme, D. The role of cathepsins in osteoporosis and arthritis: rationale for the design of new therapeutics. *Adv. Drug Delivery Rev.* **2005**, *57*, 973–993.
- (6) Felson, D. T. Osteoarthritis of the knee. *N. Engl. J. Med.* **2006**, *354*, 841–848.
- (7) Vasiljeva, O.; Reinheckel, T.; Peters, C.; Turk, D.; Turk, V.; Turk, B. Emerging roles of cysteine cathepsins in disease and their potential as drug targets. *Curr. Pharm. Des.* **2007**, *13*, 387–403.
- (8) Gauthier, J. Y.; Chaurat, N.; Cromlish, W.; Desmarais, S.; Duong, L. T.; Falguyret, J.; Kimmel, D. B.; Lamontagne, S.; Leger, S.; LeRiche, T.; Li, C. S.; Masse, F.; McKay, D. J.; Nicoll-Griffith, D. A.; Oballa, R. M.; Palmer, J. T.; Percival, M. D.; Riendeau, D.; Robichaud, J.; Rodan, G. A.; Rodan, S. B.; Seto, C.; Therien, M.; Truong, V.; Venuti, M. C.; Wesolowski, G.; Young, R. N.; Zamboni, R.; Black, W. C. The discovery of odanacatib (MK-0822), a selective inhibitor of cathepsin K. *Bioorg. Med. Chem. Lett.* **2008**, *18*, 923–928.
- (9) Eisman, J. A.; Bone, H. G.; Hosking, D. J.; McClung, M. R.; Reid, I. R.; Rizzoli, R.; Resch, H.; Verbruggen, N.; Hustad, C. M.; Da, S.,

Carolyn; Petrovic, R.; Santora, A. C.; Ince, B. A.; Lombardi, A. Odanacatib in the treatment of postmenopausal women with low bone mineral density: three-year continued therapy and resolution of effect. *J. Bone Miner. Res.* **2011**, *26*, 242–251.

(10) Stoch, S. A.; Zajic, S.; Stone, J.; Miller, D. L.; Van, D., K.; Gutierrez, M. J.; De, D., M.; Liu, L.; Liu, Q.; Scott, B. B.; Panebianco, D.; Jin, B.; Duong, L. T.; Gottesdiener, K.; Wagner, J. A. Effect of the cathepsin K inhibitor odanacatib on bone resorption biomarkers in healthy postmenopausal women: two double-blind, randomized, placebo-controlled phase I studies. *Clin. Pharmacol. Ther. (N. Y., NY, U. S.)* **2009**, *86*, 175–182.

(11) Update on phase III trial for odanacatib, Merck's investigational Cat-K inhibitor for osteoporosis. Press release, 2012. http://www.merck.com/newsroom/news-release-archive/research-and-development/2012_0711.html.

(12) Dossetter, A. G.; Beeley, H.; Bowyer, J.; Cook, C. R.; Crawford, J. J.; Finlayson, J. E.; Heron, N. M.; Heyes, C.; Highton, A. J.; Hudson, J. A.; Jestel, A.; Kenny, P. W.; Krapp, S.; Martin, S.; MacFaul, P. A.; McGuire, T. M.; Gutierrez, P. M.; Morley, A. D.; Morris, J. J.; Page, K. M.; Ribeiro, L. R.; Sawney, H.; Steinbacher, S.; Smith, C.; Vickers, M. (1*R*,2*R*)-*N*-(1-Cyanocyclopropyl)-2-(6-methoxy-1,3,4,5-tetrahydropyrido[4,3-*b*]indole-2-carbonyl)cyclohexanecarboxamide (AZD4996): a potent and highly selective cathepsin K inhibitor for the treatment of osteoarthritis. *J. Med. Chem.* **2012**, *55*, 6363–6374.

(13) Dossetter, A. G.; Bowyer, J.; Cook, C. R.; Crawford, J. J.; Finlayson, J. E.; Heron, N. M.; Heyes, C.; Highton, A. J.; Hudson, J. A.; Jestel, A.; Krapp, S.; MacFaul, P. A.; McGuire, T. M.; Morley, A. D.; Morris, J. J.; Page, K. M.; Ribeiro, L. R.; Sawney, H.; Steinbacher, S.; Smith, C. Isosteric replacements for benzothiazoles and optimization to potent cathepsin K inhibitors free from hERG channel inhibition. *Bioorg. Med. Chem. Lett.* **2012**, *22*, 5563–5568.

(14) Lecaille, F.; Kaleta, J.; Brömme, D. Human and parasitic papain-like cysteine proteases: their role in physiology and pathology and recent developments in inhibitor design. *Chem. Rev.* **2002**, *102*, 4459–4488.

(15) Wijkmans, J.; Gossen, J. Inhibitors of cathepsin K: a patent review (2004–2010). *Expert Opin. Ther. Pat.* **2011**, *21*, 1611–1629.

(16) Cai, J.; Jamieson, C.; Moir, J.; Rankovic, Z. Cathepsin K inhibitors, 2000–2004. *Expert Opin. Ther. Pat.* **2005**, *15*, 33–48.

(17) Oballa, R. M.; Truchon, J.; Bayly, C. I.; Chaurat, N.; Day, S.; Crane, S.; Berthelette, C. A generally applicable method for assessing the electrophilicity and reactivity of diverse nitrile-containing compounds. *Bioorg. Med. Chem. Lett.* **2007**, *17*, 998–1002.

(18) MacFaul, P. A.; Morley, A. D.; Crawford, J. J. A simple in vitro assay for assessing the reactivity of nitrile containing compounds. *Bioorg. Med. Chem. Lett.* **2009**, *19*, 1136–1138.

(19) Li, C. S.; Deschenes, D.; Desmarais, S.; Falguyret, J.; Gauthier, J. Y.; Kimmel, D. B.; Leger, S.; Masse, F.; McGrath, M. E.; McKay, D. J.; Percival, M. D.; Riendeau, D.; Rodan, S. B.; Therien, M.; Truong, V.; Wesolowski, G.; Zamboni, R.; Black, W. C. Identification of a potent and selective non-basic cathepsin K inhibitor. *Bioorg. Med. Chem. Lett.* **2006**, *16*, 1985–1989.

(20) Crane, S. N.; Black, W. C.; Palmer, J. T.; Davis, D. E.; Setti, E.; Robichaud, J.; Paquet, J.; Oballa, R. M.; Bayly, C. I.; McKay, D. J.; Somoza, J. R.; Chaurat, N.; Seto, C.; Scheiget, J.; Wesolowski, G.; Masse, F.; Desmarais, S.; Ouellet, M. β -Substituted cyclohexanecarboxamide: a nonpeptidic framework for the design of potent inhibitors of cathepsin K. *J. Med. Chem.* **2006**, *49*, 1066–1079.

(21) Falguyret, J.; Desmarais, S.; Oballa, R.; Black, W. C.; Cromlish, W.; Khougaz, K.; Lamontagne, S.; Masse, F.; Riendeau, D.; Toulmond, S.; Percival, M. D. Lysosomotropism of basic cathepsin K inhibitors contributes to increased cellular potencies against off-target cathepsins and reduced functional selectivity. *J. Med. Chem.* **2005**, *48*, 7535–7543.

(22) Black, W. C.; Percival, M. D. The consequences of lysosomotropism on the design of selective cathepsin K inhibitors. *ChemBioChem* **2006**, *7*, 1525–1535.

(23) Luker, T.; Bonnert, R.; Brough, S.; Cook, A. R.; Dickinson, M. R.; Dougall, I.; Logan, C.; Mohammed, R. T.; Paine, S.; Sangane, H. J.; Sargent, C.; Schmidt, J. A.; Teague, S.; Thom, S. Substituted indole-

l-acetic acids as potent and selective CRTh2 antagonists—discovery of AZD1981. *Bioorg. Med. Chem. Lett.* **2011**, *21*, 6288–6292.

(24) Ratcliffe, A. J. Medicinal chemistry strategies to minimize phospholipidosis. *Curr. Med. Chem.* **2009**, *16*, 2816–2823.

(25) Organ, M. G.; Abdel-Hadi, M.; Avola, S.; Dubovyk, I.; Hadei, N.; Kantchev, E. A.; O'Brien, C. J.; Sayah, M.; Valente, C. Pd-catalyzed aryl amination mediated by well defined, N-heterocyclic carbene (NHC)-Pd precatalysts, PEPPSI. *Chemistry* **2008**, *14*, 2443–2452.

(26) Crawford, J. J.; Dossetter, A. G.; Finlayson, J. E.; Heron, N. M. WO2009001127A1, 2008.

(27) Dossetter, A. G. A statistical analysis of in vitro human microsomal metabolic stability of small phenyl group substituents, leading to improved design sets for parallel SAR exploration of a chemical series. *Bioorg. Med. Chem.* **2010**, *18*, 4405–4414.

(28) Lewis, M. L.; Cucurull-Sanchez, L. Structural pairwise comparisons of HLM stability of phenyl derivatives: Introduction of the Pfizer metabolism index (PMI) and metabolism-lipophilicity efficiency (MLE). *J. Comput. -Aided Mol. Des.* **2009**, *23*, 97–103.

(29) Scott, J. S.; Birch, A. M.; Brocklehurst, K. J.; Broo, A.; Brown, H. S.; Butlin, R. J.; Clarke, D. S.; Davidsson, Ö; Ertan, A.; Goldberg, K.; Groombridge, S. D.; Hudson, J. A.; Laber, D.; Leach, A. G.; MacFaul, P. A.; McKerrecher, D.; Pickup, A.; Schofield, P.; Svensson, P. H.; Sörme, P.; Teague, J. Use of small-molecule crystal structures to address solubility in a novel series of G protein coupled receptor 119 agonists: optimization of a lead and in vivo evaluation. *J. Med. Chem.* **2012**, *55*, 5361–5379.

(30) Griffen, E.; Leach, A. G.; Robb, G. R.; Warner, D. J. Matched molecular pairs as a medicinal chemistry tool. *J. Med. Chem.* **2011**, *54*, 7739–7750.

(31) Testa, B.; Pedretti, A.; Vistoli, G. Reactions and enzymes in the metabolism of drugs and other xenobiotics. *Drug Discovery Today* **2012**, *17*, 549–560.

(32) Kalgutkar, A. S.; Nguyen, H. T. Identification of an N-methyl-4-phenylpyridinium-like metabolite of the antidiarrheal agent loperamide in human liver microsomes: underlying reason(s) for the lack of neurotoxicity despite the bioactivation event. *Drug Metab. Dispos.* **2004**, *32*, 943–952.

(33) Walsh, J. S.; Miwa, G. T. Bioactivation of drugs: risk and drug design. *Annu. Rev. Pharmacol. Toxicol.* **2011**, *51*, 145–167.

(34) Wen, B.; Fitch, W. L. Analytical strategies for the screening and evaluation of chemically reactive drug metabolites. *Expert Opin. Drug Metab. Toxicol.* **2009**, *5*, 39–55.

(35) Kalgutkar, A. S.; Vaz, A. D.; Lame, M. E.; Henne, K. R.; Soglia, J.; Zhao, S. X.; Abramov, Y. A.; Lombardo, F.; Collin, C.; Hendsch, Z. S.; Hop, C. E. Bioactivation of the nontricyclic antidepressant nefazodone to a reactive quinone-imine species in human liver microsomes and recombinant cytochrome P450 3A4. *Drug Metab. Dispos.* **2005**, *33*, 243–253.

(36) Kenny, P. W. Hydrogen bonding, electrostatic potential, and molecular design. *J. Chem. Inf. Model.* **2009**, *49*, 1234–1244.

(37) Toulmin, A.; Wood, J. M.; Kenny, P. W. Toward prediction of alkane/water partition coefficients. *J. Med. Chem.* **2008**, *51*, 3720–3730.

(38) Woods, K. W.; Fischer, J. P.; Claiborne, A.; Li, T.; Thomas, S. A.; Zhu, G.; Diebold, R. B.; Liu, X.; Shi, Y.; Klinghofer, V.; Han, E. K.; Guan, R.; Magnone, S. R.; Johnson, E. F.; Bouska, J. J.; Olson, A. M.; Jong, R. d.; Oltersdorf, T.; Luo, Y.; Rosenberg, S. H.; Giranda, V. L.; Li, Q. Synthesis and SAR of indazole-pyridine based protein kinase B/Akt inhibitors. *Bioorg. Med. Chem.* **2006**, *14*, 6832–6846.

(39) Boström, J.; Hogner, A.; Llinàs, A.; Wellner, E.; Plowright, A. T. Oxadiazoles in medicinal chemistry. *J. Med. Chem.* **2012**, *55*, 1817–1830.

(40) Becke, A. D. A new mixing of Hartree-Fock and local-density-functional theories. *J. Chem. Phys.* **1993**, *98*, 1372–1377.

(41) Lee, C.; Yang, W.; Parr, R. G. Development of the Colle-Salvetti correlation-energy formula into a functional of the electron density. *Phys. Rev. B: Condens. Matter* **1988**, *37*, 785–789.